



HAL
open science

Reconstruction of historical suspended particulate matter contributions of Rhône River tributaries to the Mediterranean Sea

C Bégorre, A Dabrin, M Masson, B Mourier, F Eyrolle, H Lepage, A Morereau, M Coquery

► **To cite this version:**

C Bégorre, A Dabrin, M Masson, B Mourier, F Eyrolle, et al.. Reconstruction of historical suspended particulate matter contributions of Rhône River tributaries to the Mediterranean Sea. *Geomorphology*, 2022, 417, pp.108445. 10.1016/j.geomorph.2022.108445 . hal-03816201

HAL Id: hal-03816201

<https://hal.inrae.fr/hal-03816201>

Submitted on 15 Oct 2022

HAL is a multi-disciplinary open access archive for the deposit and dissemination of scientific research documents, whether they are published or not. The documents may come from teaching and research institutions in France or abroad, or from public or private research centers.

L'archive ouverte pluridisciplinaire **HAL**, est destinée au dépôt et à la diffusion de documents scientifiques de niveau recherche, publiés ou non, émanant des établissements d'enseignement et de recherche français ou étrangers, des laboratoires publics ou privés.

Reconstruction of historical suspended particulate matter contributions of Rhône River tributaries to the Mediterranean Sea

Begorre C¹, Dabrin A¹, Masson M¹, Mourier B², Eyrolle F³, Lepage H³, Morereau A³, Coquery M¹

¹INRAE, RiverLy, F-69625, Villeurbanne, France

²Université de Lyon, UMR5023 LEHNA, Université Lyon 1, ENTPE, CNRS, 3 rue Maurice Audin, 69518 Vaulx-en-Velin, France

³Institut de Radioprotection et de Sûreté Nucléaire (IRSN), PSE-ENV, SRTE/LRTA, BP 3, Saint-Paul-lez-Durance, France

Keywords: sediment fingerprinting, trace metals, non-reactive fraction, sediment core, floods

Highlights:

Reconstruction of historical SPM inputs of the Rhône River to the Mediterranean Sea

Influence of past anthropogenic inputs on source contribution modelling

Non-reactive fraction successfully estimated past SPM inputs

Geochemical (mixing) model results are consistent with documented past flood events

1. Introduction

1 An excess of suspended particulate matter (SPM) in rivers can cause environmental and economic
2 damages (e.g., clogging spawning beds, degrading water quality or filling reservoirs; Navratil et al.,
3 2012; Torres-Astorga et al., 2018). Since the 1970s, sediment fingerprinting approaches have been
4 widely used to identify the SPM sources. Most fingerprinting studies in the literature use geochemical
5 tracers, such as trace and major elements, to assess contemporary SPM inputs in rivers. However, few
6 studies have focused on historical sediment inputs over a larger time-scale using the fingerprinting
7 approach on sediment cores, which can provide retrospective information on past hydrological events
8 (floods) or modifications of SPM fluxes, such as dam construction, bank stabilization or revegetation
9

10 (Collins et al., 1997; Navratil et al., 2012). Manjoro et al. (2017) studied several methodological factors
11 related to the work on sediment cores, such as the spatial representativeness of a sediment core, the
12 number of tracers selected and the optimal number of model iterations, on model estimations of source
13 contributions. Other studies investigated the application of geochemical (Collins et al., 1997; Pulley et
14 al., 2015), colorimetric (Pulley et al., 2018), magnetic (Pulley et al., 2015) and radiometric (Pulley et
15 al., 2015) tracers for estimating source contributions of contemporary SPM in a sediment core; this was
16 done for periods ranging from a few decades to 250 yr. The main objectives of fingerprinting studies
17 applied on sediment cores are to investigate changes in SPM sources over time (Collins et al., 1997;
18 Manjoro et al., 2017). The results were interpreted by comparing estimates of the historical source
19 contributions against information related to land-use changes (Huang et al., 2019), reservoir construction
20 (Gateuille et al., 2019), implementation of actions to reduce soil erosion (Wang et al., 2018), or available
21 hydrological data (Navratil et al., 2012).

22 The reconstruction of historical SPM inputs into a river generally implies measurements of tracers in
23 contemporary SPM used as source samples. However, Pulley et al. (2015) is one of the few studies that
24 reported the risk of using non-conservative tracers (e.g., changes in organic matter content, particle size
25 selectivity, geochemical and magnetic reactions along the sedimentary profile) to assess historical
26 source contributions in sediment cores. Begorre et al. (2021) recently showed that the main issue with
27 using fingerprinting approaches on sediment cores is the non-conservative behaviour of the geochemical
28 tracers (i.e., total trace and major elements) because (i) tracers undergo diagenetic processes that modify
29 their partitioning and concentrations in sediment layers, and (ii) tracers have been largely modified since
30 the mid-1970s, notably because of changes in anthropogenic inputs (Audry et al., 2004; Dhivert et al.,
31 2016). The proposed alternative was to use the non-reactive fraction to limit the effects of non-
32 conservative behaviour of the selected tracers. One advantage of this novel approach is that it increases
33 the number of conservative tracers available after passing the range test (Begorre et al., 2021).

34 Focusing on the Rhône River, historical sediment contamination by polychlorobiphenyls and metals
35 (Mourier et al., 2014; Dendeviel et al., 2020) and contributions from contemporary sources of SPM
36 across the river catchment (Zebracki et al., 2015; Dabrin et al., 2021) have previously been documented.

37 At the scale of the Bléone River, which is a sub-catchment of the Durance River (a tributary of the
38 Rhône River), Navratil et al. (2012) reconstructed the geological sources of SPM over time via the
39 analysis of a sediment core study using radionuclide and geochemical tracers. However, to date, no
40 study has documented historical SPM contributions of the main Rhône River tributaries to the river
41 outlet. Zebracki et al. (2015) quantified the contributions of three main SPM sources, which included
42 tributaries grouped according to hydrological characteristics (Cévenol, Oceanic and Mediterranean
43 rivers), and used radionuclide data to show that the Durance River is the main relative contributor of
44 SPM at the outlet of the Rhône River. Interest in the study of the sources of sediments on the Rhône
45 River is based on the major sedimentary contributions of the Rhône River to the Mediterranean Sea
46 (Delile et al., 2020). Given that fine sediments affect water quality and aquatic biodiversity (Koiter et
47 al., 2013), it is essential to identify sediment sources to reduce sediment inputs to the Mediterranean
48 Sea. Dendeviel et al. (2020) have worked on historical metal contamination along the Rhône River
49 continuum; but, to the best of our knowledge, no studies have been published on historical sediment
50 sources to the Mediterranean Sea.

51 In this context, the main objective of the present study was to highlight the relevance of using tracers in
52 the non-reactive fraction to retrace the historical SPM contributions of the main tributaries of the Rhône
53 River basin to its global SPM discharge to the Mediterranean Sea over the last 40 yr. This study is based
54 on the collection and analysis of a sediment core located close to the outlet of the Rhône River basin,
55 which is only connected to the main channel during major flood events, and on SPM samples collected
56 within the Rhône Sediment Observatory (OSR) monitoring network, which has been operational since
57 2012. To overcome the methodological biases resulting from changes in anthropogenic inputs and
58 diagenetic processes potentially affecting concentrations of trace and major elements in sediment cores,
59 we applied an original fingerprinting method based on the analysis of the non-reactive fraction of
60 elements. This fingerprinting approach was previously used by Begorre et al. (2021) on a sediment core
61 sampled on the Upper Rhône River, but the depth resolution of the sediment core was too limited to
62 investigate sediment inputs at the flood-event scale, in contrast to the sediment core collected
63 downstream of the Rhône River basin for the present study.

64

65 2. Material and Methods

66 2.1. Study area: the Rhône River basin

67 The Rhône River is one of Europe's major rivers and the largest supplier of sediments to the
68 Mediterranean Sea, delivering an inter-annual mean of 5.5 Mt yr⁻¹ over the 2008–2018 period (Delile et
69 al., 2020). The basin covers an area of 95,600 km² spanning a broad diversity of geological and climatic
70 conditions (Zebracki et al., 2015; Delile et al., 2020). Over the last 40 yr, eight major flooding events
71 were reported at the Beaucaire station close to the outlet of the Rhône River basin: in 1982 (maximum
72 water discharge, $Q_{\max} = 8025 \text{ m}^3 \text{ s}^{-1}$), 1990 ($Q_{\max} = 5300 \text{ m}^3 \text{ s}^{-1}$), 1993 ($Q_{\max} = 9800 \text{ m}^3 \text{ s}^{-1}$), 1994
73 ($Q_{\max} = 11,006 \text{ m}^3 \text{ s}^{-1}$), 1996 ($Q_{\max} = 8981 \text{ m}^3 \text{ s}^{-1}$), 1997 ($Q_{\max} = 8020 \text{ m}^3 \text{ s}^{-1}$), 2002 ($Q_{\max} = 9700 \text{ m}^3 \text{ s}^{-1}$)
74 and 2003 ($Q_{\max} = 11,500 \text{ m}^3 \text{ s}^{-1}$) (DREAL, 2011). Concentrations and fluxes of SPM and associated
75 contaminants are monitored in the Rhône River and its main tributaries under the Rhône Sediment
76 Observatory (“OSR”) program (Fig. 1). A monitoring network that has been set up and running since
77 2009 collects a large set of SPM samples and data via stations located across the entire basin (Thollet et
78 al., 2021). The study area includes eleven tributaries located upstream of the sediment core location near
79 the Rhone River outlet (Fig. 1), i.e., the Arve, Fier, Guiers, Ain, Bourbre, Saône, Gier, Isère, Ardèche,
80 Durance and Gardon rivers.

81

82 2.2. Sampling strategy

83 2.2.1. Suspended particulate matter source sampling

84 The SPM samples were collected at five river stations representing the potential SPM sources to
85 characterize geochemical signatures of sediment sources: the Middle Rhône River at the Andancette
86 station (including inputs from seven tributaries, i.e., the Arve, Fier, Guiers, Ain, Bourbre, Saône and
87 Gier rivers), the Isère, Ardèche, Durance and Gardon river stations (Fig. 1). The Andancette station is
88 located on the Rhône River, upstream of its confluence with the Isère River. The other stations are
89 located downstream of each tributary, at a few kilometres upstream from their confluence with the

90 Rhône River (Thollet et al., 2021). The SPM samples were collected using integrative particle traps
91 deployed throughout the year and retrieved every month. In order to collect SPM samples during specific
92 events, such as the Cévenol floods, event-based samplings were carried out using a continuous flow
93 centrifuge (Westfalia KA 2-86-76) or by manually sampling large volumes of water. A more detailed
94 description of the sampling methods can be found in Masson et al. (2018). Overall, 42 SPM samples
95 were collected between 2011 and 2019 from five sources: the Middle Rhône River (n=11), the Isère
96 River (n=14), the Ardèche River (n=6), the Gardon River (n=2) and the Durance River (n=9) (see Table
97 1).

98 2.2.2. Targeted sediment core sampling

99 To assess the historical SPM inputs from Rhône River tributaries, a 300-cm-long sediment master core
100 was reconstructed by combining seven individual sediment cores collected from two holes (16 cm apart)
101 at different depths at the Mas des Tours site, which is located 54 km upstream of the Mediterranean Sea
102 (43.740000 N; 4.625194 E; Fig. 1), in May 2018 (Morereau et al., 2020). This sampling site was selected
103 because it is only connected to the Rhône River during major floods events. Core drilling was carried
104 out using a Cobra TT percussion driller equipped with a transparent 90-mm diameter PVC liner. Using
105 a XRF core scanner (ITRAX, Cox Analytical Systems, Sweden), 43 layers ranging in thickness from 2–
106 15 cm were identified. Each layer was subsampled using a ceramic knife to collect several grams of
107 fresh sediment. A subsample was stored for particle size analysis. Other sediment subsamples were
108 freeze-dried, ground, and stored in plastic bags until further analysis. All information about core dating
109 are fully reported and discussed by Morereau et al. (2020).

110

111 2.3. Physicochemical analysis of SPM and sediment samples

112 The particle size distribution was determined on fresh SPM samples using a Cilas 1190 particle size
113 analyzer under ultrasound and sample agitation, according to ISO standard 13320 (ISO, 2009). For the
114 sediment core samples, the particle size distribution was determined on a Mastersizer 2000© instrument
115 (Malvern Panalytical, Instruments Ltd., Malvern, UK) with a small-volume wet dispersion unit. Tests

116 carried out to compare results obtained by these two instruments showed that there are no significant
117 differences between the results.

118 The analysis of geochemical properties involved the quantification of 20 trace and major elements
119 (metals) in the total and reactive fractions (see supplementary material “Database_Rhône_River”). As
120 highlighted by Dabrin et al. (2021), soft extraction using HCl has been used for many years to identify
121 metals adsorbed on the reactive fraction of SPM, which is mainly present in anthropized systems. The
122 total fraction was determined after triacid mineralization (12 M hydrochloric acid, 14 M nitric acid and
123 22 M hydrofluoric acid, respectively proportioned at 1.5 mL, 0.5 mL and 2 mL) on a heating plate. The
124 reactive fraction was obtained by soft extraction using hydrochloric acid (1 M) at room temperature
125 (Dabrin et al., 2014). The difference between the concentrations of the two fractions correspond to what
126 we call a ‘non-reactive fraction’. Further details can be found in Begorre et al. (2021). Major and trace
127 elements were analyzed in both fractions by inductively-coupled plasma optical emission spectroscopy
128 (ICP-OES, Agilent 720-ES) or triple-quadrupole inductively-coupled plasma mass spectrometry (TQ-
129 ICP-MS, Thermo iCAP-TQ) according to their limit of quantification and concentration in the samples.
130 Certified reference materials (IAEA-158, marine sediment for total extraction, and LGC-6187, river
131 sediment) were analyzed in triplicates for each analytical series to control the accuracy of results.
132 Precision was lower than 11% for each element analyzed. When considering sediment samples,
133 precision of the analysis by ICP-OES was similar between the total and HCl fractions with values in the
134 range of 0.3-9.7% depending on the metal. For analysis by ICP-MS, analytical precision on triplicates
135 was lower than 7% for the total fraction against lower than 9% for the HCl fraction. In addition, blanks
136 were systematically included in the mineralization and analytical series to confirm that the samples were
137 not contaminated during the analytical process.

138

139 2.4. Sediment core dating

140 Sediment core dating was performed according to the procedure detailed in Morereau et al. (2020).
141 Briefly, the sediment core could not be dated with the traditional markers such as ^{137}Cs and ^{210}Pb s

142 (Appleby, 1998; Foucher et al., 2021). In fact, the Marcoule nuclear facility located along the Rhône
143 River also releases those radionuclides into the waters in proportion that diluted the contributions of the
144 watershed and masked the traditional markers (Provansal et al., 2010). For this reason, the dating of this
145 archive was carried out by modelling using the data on the releases from this facility (Morereau et al.,
146 2020). Dry samples of sediment were conditioned in 17-mL or 60-mL boxes depending on the quantity
147 of sediment available and were placed in vacuum-sealed packages and stored for at least one month
148 before analysis to ensure the secular equilibrium of the ^{210}Pb necessary to determine the concentration
149 of ^{210}Pb xs (Morereau et al., 2020). Measurements of gamma emitters were performed with a germanium
150 detector. Dating was confirmed using additional information input, such as the chronology of past
151 flooding events. Morereau et al. (2020) showed that, because of the location of the coring site, the
152 deposited sediments mainly correspond to flood deposits. Dating of the sediment core showed that the
153 43 layers included sediments deposited from 1981 to 2017. The mean apparent sedimentation rate was
154 estimated at 7.8 cm yr^{-1} .

155

156 2.5. Statistical analysis and fingerprinting procedure

157 2.5.1. Data treatment before implementation in the geochemical (mixing) model

158 Trace and major element concentrations in the total or residual (non-reactive) fraction were corrected
159 for differences in particle size between the SPM sources and the sediment core. The correction method
160 applied was the method described by Gellis and Noe (2013) and implied a particle size difference
161 between SPM from tributaries (source samples) and the sediment core (target samples). As illustrated
162 in Supplementary Information SI.1, the SPM of the Ardèche and Durance rivers had significantly
163 different D_{50} values (median value of the particle size distribution) than the sediment core samples. For
164 metals that correlate positively with D_{50} values, concentrations were corrected according to Eq. (1):

$$165 C_f = C_i - [D50_{(S)} - D50_{m(\text{Sed})}] \times p \quad (1)$$

166 where C_f is corrected concentration of tracer i , C_i is initial concentration of tracer i in source s , $D50_{(s)}$
167 is median particle size value of source s , $D50_{m(Sed)}$ is average D_{50} value for all target sediment samples,
168 and p is slope of the regression line.

169 Trace and major elements integrated in the geochemical model were selected by a three-step
170 procedure: a range test to keep conservative metals (Eq. (2)), a Kruskal-Wallis test to remove
171 redundant elements, and a discriminant factor analysis (DFA) to determine the signature that ensures
172 optimal source discrimination. Results of this tracer selection process are reported in Table 2.

$$173 \quad [\min(C_{is})]_{\text{mean}} - 0.10 \times [\min(C_{is})]_{\text{mean}} < C_i < [\max(C_{is})]_{\text{mean}} - 0.10 \times [\max(C_{is})]_{\text{mean}} \quad (2)$$

174 where C_{is} is concentration of tracer i in source s , and C_i is concentration of tracer i in sediment core
175 layers. The concentration of tracer i in the sediment core must lie within the source range represented
176 by the minimum and maximum concentrations of tracer i in sources for which a 10% error is accepted.

177 The distribution-mixing model coupled to Monte Carlo simulation resolved Eq. (3) to estimate the
178 source contributions with their associated uncertainties from the selected tracers for each layer of the
179 sediment core. Uncertainties associated with the source contributions were calculated based on 95%
180 confidence interval and mean absolute error (MAE; Eq. 4).

$$181 \quad C_i = \sum_{l=1}^{1000} \sum_{s=1}^n (P_s \times C_{is}) / 1000 \quad (3)$$

182 where P_s is percentage contribution from SPM tributary s , C_{is} is concentration of tracer i in tributary s ,
183 n is number of tributaries, and C_i is tracer concentration in the target sediment samples (Hughes et al.,
184 2009; Haddadchi et al., 2013). Note that this model is based on two conditions: the source
185 contributions should be between 0 and 100%, and the sum of the contributions is equal to 100%
186 (Hughes et al., 2009; Navratil et al., 2012; Collins et al., 2017).

$$187 \quad MAE = 1 - (\sum_{i=1}^m |C_i - (\sum_{s=1}^n P_s \times C_{si})| / C_i) / m \quad (4)$$

188 where m is number of properties. If the MAE is greater than 0.85, then the model results are reliable.

189 **2.5.2. Statistical tests to investigate metal reactivity in the sediment cores**

190 To investigate metal reactivity in the sediment profile, a Student's *t*-test or Wilcoxon test was used to
191 compare tracer concentrations between total and non-reactive fractions of SPM, concentrations
192 between tributaries, and concentrations of metals between top (1991–2017 period) and bottom (1981–
193 1990 period) layers of the sediment core. The level of significance used in statistical tests was set at a
194 p -value < 0.05 .

195 **3. Results and Discussion**

196 3.1. Reactivity of tracers in SPM and sediment core from the Rhône River basin

197 Total and non-reactive metal concentrations in SPM for each studied tributary are reported in Fig. 2.
198 The two layers corresponding to sediment deposited in 2014 and 2017 were removed from further
199 analysis because the non-reactive concentrations of 7 out of the 12 metals analyzed were below the
200 limit of quantification, which could narrow the applicability of the fingerprinting method by
201 decreasing the number of available tracers. The study reported here therefore considers the 1981–2013
202 period. To apply a robust fingerprinting method, it is necessary to select metals with low or moderate
203 reactivity in SPM for all tributaries and in the sediment core. To investigate the spatial (contemporary
204 SPM) and temporal (sediment core) variability in metal reactivity, we assessed metal reactivity
205 according to percentage of reactive fraction to percentage of total fraction (see Table 2). Based on
206 these percentages, we categorized the trace and major elements into three groups: low reactivity
207 ($< 20\%$), moderate reactivity (20% – 50%) and high reactivity ($>50\%$). The percentages listed in Table
208 2 were determined from the mean percentage values of all samples for each tributary. Only two
209 samples were available for the Gardon River, and so we were unable to reach a definitive conclusion
210 on metal reactivity for this tributary.

211 Begorre et al. (2021) found that all groups of metals in the Upper Rhône River presented the same
212 reactivity in SPM across all the studied tributaries: Al, Cr, Ti and V displayed low reactivity, Co and
213 Ni had moderate reactivity, and Cu, Mn and Sr showed strong reactivity. Here we found a globally
214 similar pattern of results, although the SPM from the Ardèche and Durance rivers had the highest
215 reactive fractions of most metals compared to other tributaries. In addition, the reactivity group of Ba,

216 Fe and Zn varied according to the source considered, whereas Al, Co, Cr, Cu, Mn, Ni, Sr, Ti and V
217 were assigned to the same reactivity group whatever the tributary considered. For example, Ba showed
218 low reactivity in SPM at the Andancette (Middle Rhône River) and Isère river stations (18% and 19%,
219 respectively), whereas it was moderately reactive in the Ardèche and Durance rivers (32% and 40%,
220 respectively). Iron also showed spatial variability in its reactivity, with low reactivity in SPM from the
221 Isère River (19%), but moderate reactivity for SPM collected at the Andancette, Ardèche and Durance
222 rivers (30%–31%). Finally, Zn showed moderate reactivity in SPM from the Isère and Durance rivers
223 (33% and 43%, respectively), whereas it was highly reactive in SPM from the Andancette (56%) and
224 Ardèche (65%) rivers. This higher reactivity of Zn at the Andancette and Ardèche river stations could
225 be explained by Zn pollution caused by numerous anthropogenic activities, i.e., by vineyards and
226 industries along the Middle Rhône River, and by farming and old mining tailings on the Ardèche
227 River (Ollivier et al., 2011; Dendeviel et al., 2020).

228 Metal concentrations in the sediment core displayed different temporal patterns (Fig. 3). Based on
229 linear regression (i.e., data not shown), total concentrations of Al, Ti, V, Mn, Ni, Co, Sr and Fe did not
230 show a significant trend from the deepest layers through to the top of the sediment core. In contrast,
231 Cr, Cu, Zn and Ba concentrations in the total sediment fraction decreased from 1981 to 2013
232 (statistically significant linear regression with $R^2_{Cr}=0.67$ and $p<0.05$, $R^2_{Cu}=0.65$ and $p<0.05$, $R^2_{Zn}=0.67$
233 and $p<0.05$, $R^2_{Ba}=0.78$ and $p<0.05$). In detail, total Cu, Zn, Cr and Ba concentrations before 1990
234 differed significantly from concentrations measured after 1990, and they all followed a decreasing
235 trend in the total fraction from 1981 to 1990 (Fig. 3). For Cr and Ba, this temporal trend is also
236 highlighted for non-reactive concentrations, which could mean that Cr and Ba were not influenced by
237 past anthropogenic inputs. Conversely, non-reactive concentrations of Cu and Zn did not vary over
238 time and were significantly different from their total concentrations, suggesting that only the reactive
239 fraction of Cu and Zn decreased over time (from 1981 to 1990), which could be explained by
240 historical anthropogenic inputs of reactive metals. This decrease in total Zn concentrations is
241 consistent with Zn concentrations in the sediment core (Ferrand et al., 2012) and surface sediments
242 from the National Basin Network of the French Water Agency, which highlighted a decreasing trend

243 from 1986 to 1990 (Ferrand et al., 2012). Furthermore, Dendeviel et al. (2020) highlighted (i) that Cu
244 and Zn were delivered all along the Rhône River by multiple anthropogenic activities (i.e., vineyards,
245 mining, cable production, a nuclear power plant, the Marcoule reprocessing spent fuel facility) in the
246 1980s, and (ii) that Cu and Zn concentrations decreased from 1960 to 1990. Moreover, Morereau et al.
247 (2020) reported that the Marcoule facility (on the Rhône River, just north of the Durance tributary)
248 released liquid effluents highly contaminated with Cu and Zn until 1990. Based on these observations,
249 we supposed that some metals are more reactive in the deepest sediment core layers (1981–1990)
250 compared to the more recent layers (1991–2013). We therefore scrutinized metal concentrations in the
251 sediment core separately for these two periods, i.e., 1981–1990 and 1991–2013.

252 Concentrations of Al, Ti, V, Mn, Ni, Co, Sr, Fe, Cr and Ba measured in the non-reactive fraction co-
253 evolved with the total fraction over time, whereas concentrations of Cu and Zn in the non-reactive
254 fraction remained stable along the sediment core. This means that the total concentrations of these two
255 elements may be influenced by variable anthropogenic inputs or variable reactivity, which makes them
256 unreliable for tracing historical sediment sources. This is supported by our metal reactivity study based
257 on proportions of the reactive fraction, which classified all metals except Zn into the same reactivity
258 groups whatever the sediment core layer considered. Indeed, Zn showed moderate reactivity in the
259 upper part of the core (50%) but was highly reactive in the deepest layers (1981–1990) of the sediment
260 core (63%). Begorre et al. (2021) also showed that, in a sediment core sampled in the Upper Rhône
261 River, the reactive fraction of Zn was higher before the 1990 layer (80%) compared to the more recent
262 layers (66% for the 1991–2013 period).

263 Metal reactivity could also differ between SPM tributaries and the sediment core. Al, Co, Cr, Cu, Mn,
264 Ni, Sr, Ti and V showed the same degree of reactivity in SPM tributaries and the sediment core, which
265 is consistent with results obtained by Begorre et al. (2021) for the sediment core sampled in the Upper
266 Rhône River. However, Sr showed significant differences between the highest reactive fraction in
267 SPM from the Durance River (89%) and all other stations (~65%). The reactive fraction of Sr
268 determined in the sediment core layers was similar between the top and bottom of the core at values of
269 around 74–76%. These results showed that SPM from the Durance River were characterized by a

270 higher Sr reactivity than sediment core layers and SPM from the other tributaries. This could be
271 explained by the high carbonate contents in SPM from the Durance River because of its sedimentary
272 basin (Ollivier et al., 2011). Ollivier et al. (2011) showed that Sr is mainly associated with carbonates,
273 which represent the most reactive fraction of particles, meaning that Sr can easily be removed from
274 particles to the dissolved phase under varying physicochemical conditions. They also highlighted that
275 the Rhône River drains mainly carbonate bedrocks, which are significant sources of SPM during major
276 flood events, as in the case of the 2001 and 2002 floods (Ollivier et al., 2011). These events
277 correspond to the increase in total concentrations of Sr found, in the present study, in the recent layers
278 of the core (2001–2013) collected at the outlet of the Rhône River. Liu et al. (2013) studied changes in
279 concentrations of metals associated with reducible and carbonate phases in two coastal sediment cores
280 (Taiwan) and found that metal concentrations were correlated to the carbonate content and that Sr
281 concentrations in the carbonate fraction were higher in the recent layers compared to the deepest
282 layers (Liu et al., 2013). Given that Sr has a high affinity with the carbonate fraction in the Rhône
283 River, it is consistent that total Sr concentrations were higher in the recent layers (2001–2013) of the
284 sediment core studied here.

285 The reactive fraction of Ba, Fe and Zn also differed between the sediment core and SPM samples at
286 some stations (Table 2). For example, in case of Ba, the reactive fraction measured in SPM from the
287 Isère (19%) and Andancette (18%) stations was significantly different ($p < 0.05$) than the reactive
288 fraction in the sediment core (39% and 43% for the 1981–1990 and 1991–2013 periods, respectively).
289 Conversely, the percentages of the reactive fraction of Ba in SPM from the Ardèche (32%) and
290 Durance (40%) rivers were similar to those found in the sediment core. As reported by Kresse et al.
291 (2007), the erosion of sedimentary rocks constituted by Ba-enriched carbonates could explain the
292 higher reactivity of Ba in SPM from the Ardèche and Durance rivers, in comparison to other
293 tributaries. Furthermore, comparison of our results against those obtained for the sediment core
294 sampled on the Upper Rhône (Begorre et al. 2021) shows that Ba reactivity increased downstream of
295 the watershed, i.e., from 20% for the Upper Rhône to 39%–43% at downstream sites. Ba-based
296 minerals are generally found in the non-reactive fraction of the particles, but under anoxic conditions,

297 these minerals are dissolved and then precipitate again in the sedimentary deposits (Henkel et al.,
298 2012). This may explain, depending on the presence of such minerals, the increase in the total and
299 non-reactive concentrations of Ba with depth. The spatial variation in total and non-reactive Ba
300 concentrations from the Upper Rhône (mean of 253 mg kg⁻¹ and 203 mg kg⁻¹, respectively) to the
301 Rhône River outlet (mean of 577 mg kg⁻¹ and 336 mg kg⁻¹, respectively) may be explained by a
302 missing source of dissolved Ba that precipitates under oxic conditions. Values for the reactive fraction
303 of particulate Fe were similar between the Middle Rhône (Andancette station), Ardèche and Durance
304 rivers (30–31%) and also similar to those observed in the sediment core layers deposited between
305 1991 and 2013 (32%). The SPM from the Isère River was the only exception, with a lower percent
306 reactive fraction of Fe (19%). Liu et al. (2013) highlighted that Fe is mainly associated with the oxide
307 fraction of particles. However, to validate this assumption in the case of the Rhône River, it would be
308 necessary to have information about the oxide fraction in SPM samples from each tributary. For Zn, a
309 high reactivity was found in SPM from the Ardèche River (65%), which is almost two-fold higher
310 than the lowest value measured for SPM from the Isère River (33%). This Zn reactivity in SPM of the
311 Ardèche River (65%) was similar to the Zn reactivity in the deepest layers of the sediment core (63%
312 for the 1981–1990 period). We assume that because Zn is statistically selected and used in the
313 geochemical model, the high reactivity of Zn would introduce a bias in the contribution estimates for
314 the model based on the total fraction.

315 Note that the metal reactivity investigation can serve to identify the most appropriate tracers for
316 reliably estimating source contributions. Owens et al. (2016) highlighted that the range test, which is
317 commonly used to remove non-conservative elements, is not fully reliable. This was explained by the
318 fact that (1) even if total concentrations of a tracer remain within the range values of the sources, they
319 can still evolve because of tracer reactivity and move away from initial concentrations (e.g., metal
320 precipitation in the mixing zone may lead to higher tracer concentrations), and that (2) some elements
321 were removed from the procedure because of higher concentrations from an unidentified source
322 (Owens et al., 2016). In the present study, based on the range test results, metals included in the low
323 and moderate reactivity groups (i.e., Al, Ba, Co, Cr, Fe, Ni, Ti and V) could be used to reliably trace

324 sediment sources. However, total concentrations of metals in the third (high reactivity) group (i.e., Cu,
325 Mn, Sr) are not recommended for estimating source contributions. Zn is a distinctive element as it is
326 moderately reactive at the top of the sediment core (1990–2013 period) while it is highly reactive in
327 the deeper layers (1981–1990; Table 2).

328

329 3.2. Historical reconstruction of relative contributions of SPM sources to the Rhône River

330 3.2.1. Selection of tracers in the geochemical model

331 The optimal composite signature integrated in the geochemical model was selected using the range
332 test, as detailed in Section 2.5.1. The range test results (Table 3) show that four elements (i.e., Ba, Cr,
333 Cu and Ti) were excluded from this procedure for the total fraction, and that Mn, Sr and Zn, which are
334 highly reactive, were kept for further statistical tests (Kruskal-Wallis and DFA). For the non-reactive
335 fraction, only two elements (i.e., Ba and Ti) were excluded from the fingerprinting procedure.

336 Following the range test, the tracers selected by the combination of the Kruskal-Wallis test and DFA
337 were Co, Fe, V and Zn for the total fraction, and Al, Cr, Fe, Mn and Zn for the non-reactive fraction.

338 For the total fraction, the procedure statistically selected Zn to estimate the source contributions,
339 which could influence the reliability of the results. For the non-reactive fraction, two reactive metals
340 (i.e., Mn and Zn) were integrated into the geochemical model, but the estimation of source
341 contributions based on their non-reactive concentrations made it possible to overcome problems
342 associated with metal reactivity or past anthropogenic inputs. These results are in agreement with the
343 work of Begorre et al. (2021), showing that tracer selection varied between both fractions leading to a
344 larger number of available tracers for the non-reactive fraction.

345 3.2.2. Global trends in historical SPM inputs to the Mediterranean Sea

346 Fig. 4 shows the contributions of SPM sources, expressed as percentages, estimated from tracer
347 concentrations in the total and non-reactive fractions. Overall, along the whole sediment core (1981–
348 2013), the contributions modeled from the total fraction differed significantly ($p < 0.05$) from the

349 contributions estimated using the non-reactive fraction for the Durance and Isère rivers. For example,
350 the SPM contributions of the Durance River modeled using the total and non-reactive fractions were
351 $22 \pm 13\%$ and $52 \pm 18\%$, respectively. Given that the sediment core was collected in the Rhône River
352 downstream of the confluence with the Durance, the sediment core is probably strongly influenced by
353 SPM inputs from the Durance River (Vauclin et al., 2021).

354 Source contributions modeled using the total fraction showed that the Isère and Ardèche rivers were
355 the main contributors to the SPM at the outlet of the Rhône watershed from 2013 to 1991 (27–175 cm
356 depth) and from 1990 to 1981 (184–300 cm depth), respectively. Contributions estimated using non-
357 reactive concentrations showed that the Durance River was the main source of deposited sediments
358 over time, except in layers from 1989, 1996, 1998 and 2001 for which the main SPM inputs came
359 from other tributaries (Fig. 4-b). Globally, the Middle Rhône River inputs were low and relatively
360 stable ($5.6 \pm 3.1\%$) over time, except in the layers from 1989 (37%), 2001 (19%) and 2003 (16%). In
361 the absence of historical SPM flux data, we compared our results against results from the literature
362 (Zebracki et al., 2015; Poulier et al., 2019). Zebracki et al. (2015) used radionuclide analyses to
363 investigate contemporary sources of SPM transported to the Rhône River outlet between 2001 and
364 2011, and identified three groups of tributaries: upstream (Ain, Fier, Isère, and Saône rivers); pre-
365 alpine (Durance, Drôme rivers) and Cévenol (Ardèche, Gardon rivers). The Durance River was
366 identified as the main contributor of SPM (53%), followed by the “Andancette + Isère” (35%) and
367 Cévenol rivers (11%) (Zebracki et al., 2015). The results obtained here using the non-reactive fraction
368 ($52 \pm 18\%$, $22 \pm 13\%$, and $26 \pm 16\%$, respectively) are therefore more consistent with the findings of
369 Zebracki et al. (2015) than the results obtained using the total fraction. We also compared our
370 estimates of source contributions against the relative SPM flux contributions calculated over the
371 2000–2016 period by Poulier et al. (2019) for the Middle Rhône (16%; Upper Rhône River + Saône),
372 Isère (25%), and Durance (24%) rivers. The major SPM contributors to the Mediterranean Sea were
373 the Isère and Durance rivers. According to these results, our estimates of SPM contributions based on
374 the total fraction are likely more accurate than those based on the non-reactive fraction for the 2000–
375 2016 period. However, these results should be interpreted with caution because Poulier et al. (2019)

376 did not include the Cévenol tributaries. The differences in conclusion between both comparisons
377 might be associated with the method applied to evaluate the contribution of SPM sources. Poulier et
378 al. (2019) used the SPM flux data calculated at each sub-watershed outlet without calculating relative
379 SPM proportions delivered to the Rhône River, whereas Zebracki et al. (2015) and the present study
380 compared geochemical signatures between SPM sources and sediment core layers. Zebracki et al.
381 (2015) noted the presence of a large number of dams along the Rhône River continuum, which may
382 explain the underestimated contributions from upstream tributaries. Estimates of source contributions
383 using geochemical models were therefore more representative of SPM inputs to the watershed outlet.
384 Regarding result reliability, the MAE calculated for each layer of the sediment core were higher for
385 the non-reactive fraction (average = 99.8%) than for the total fraction (average = 95.4%). Considering
386 each layer individually, it can be observed that all MAE were higher than 85%, which means that the
387 results are reliable except for the 2003 layer for the total fraction (MAE = 81%).

388 3.2.3. Temporal variations in historical SPM contributions

389 The contributions of the Andancette station estimated from total and non-reactive fractions were very
390 low and not significantly different in top ($7 \pm 3\%$ and $8 \pm 5\%$ for the total and non-reactive fractions,
391 respectively; $p=0.88$) and bottom ($4 \pm 3\%$ and $7 \pm 8\%$ for the total and non-reactive fractions,
392 respectively; $p=0.07$) layers of the sediment core. In contrast, the source contributions of the Isère,
393 Ardèche, Gardon and Durance rivers varied over time (Fig. 4).

394 Differences in source contributions between both fractions depended on the sediment core layers. For
395 the total concentrations, the contributions of SPM sources differed significantly between the top of
396 the core (from 1991 to 2013) and the deepest layers (from 1981 to 1990), whereas for the non-reactive
397 fraction, the contributions were not significantly different between both parts of the sediment core.
398 For example, in the top of the sediment core, the contributions of the Ardèche and Gardon rivers were
399 similar for those estimated based on the total fraction ($13 \pm 6\%$ and $14 \pm 13\%$, respectively) and the
400 non-reactive fraction ($15 \pm 5\%$ and $13 \pm 13\%$ respectively), whereas in the deepest layers, the
401 estimated source contributions were significantly different between fractions (total fraction: $32 \pm 16\%$
402 and $22 \pm 14\%$ for the Ardèche and Gardon rivers, respectively; non-reactive fraction: $12 \pm 3\%$ and

403 13 ± 9%, respectively). To explain these differences, a Pearson correlation test and a principal
404 component analysis (PCA) were carried out based on the tracers selected by DFA for the total (Co,
405 Fe, V, Zn) and non-reactive (Al, Cr, Fe, Mn, Zn) fractions, and results were interpreted according to
406 the geochemical model results (Fig. 5). These statistical tests showed that the contributions of the
407 Ardèche River were significantly correlated to Zn concentrations in the total fraction ($p < 0.05$; Fig. 5-
408 a). In addition, as previously demonstrated (see Section 3.1), Zn was characterized as highly reactive
409 in the 1981–1990 layers, meaning that it was influenced by past anthropogenic inputs (Dendeviel et
410 al., 2020). Consequently, the estimated increasing contributions from the Ardèche River from 1990 to
411 1981 did not reflect an increase in Ardèche River SPM inputs but instead revealed substantial historic
412 anthropogenic inputs of Zn at the global Rhône River scale, as discussed above.

413 3.2.4. Cross-analysis of relative historical SPM contributions and past flood events

414 To discuss and confront the results of the two fingerprinting approaches, we compiled the main
415 historical flood events (DREAL, 2011), and reported them in Fig. 4-c according to each identified
416 layer of the sediment core. The discussion is presented in reverse chronological order.

417 In 2010 (42 cm depth), a flood of the Isère River with a ten-year return period, i.e., a flow exceeding
418 $900 \text{ m}^3 \text{ s}^{-1}$, was recorded, which implies higher SPM inputs from the Isère River compared to the other
419 tributaries. For this layer, there was no marked peak in contributions for any particular tributary in
420 either total or non-reactive fraction, as there was no sediment deposition from this flood event at the
421 study site. For the total fraction, the Isère River SPM contribution was 39% against only 13% for the
422 non-reactive fraction. Combining the contributions of the Middle Rhône with those of the Isère River
423 for the present study, the SPM contributions modeled using the total and non-reactive fractions were
424 45% and 17% of total SPM inputs, respectively. For the Durance River, the SPM contributions
425 modeled from the total and non-reactive fractions were $36 \pm 19\%$ and $59 \pm 19\%$, respectively. Given
426 that the Durance River is much closer to the sediment core site than the Isère River (see Fig. 1), it is
427 possible that the flood peak of the Isère River was not observed at this time in the sediment core at the
428 Rhône River outlet because of SPM storage in the dam reservoir located downstream of the
429 confluence of the Isère River and the Rhône River (Zebracki et al., 2015).

430 In 2003 (96 cm depth), the deposited sediments were characterized by SPM transported during an
431 extensive Mediterranean flood implying a flood on the Durance ($1100 \text{ m}^3 \text{ s}^{-1}$) and Ardèche
432 ($2510 \text{ m}^3 \text{ s}^{-1}$) rivers. Total and non-reactive fractions showed a major contribution of the Durance
433 River of 58% and 54%, respectively, which is consistent with the hydrological data illustrated in Fig.
434 4-c (DREAL, 2011) and with Zebracki et al. (2015), who estimated contributions of the Durance River
435 at between 38% and 53% during the Mediterranean floods for the 2000–2012 period. Contributions of
436 the Ardèche River were estimated at 21% and 25% for the total and non-reactive fractions,
437 respectively. These contributions could be explained by the flood event that occurred on the Ardèche
438 River and reached a water flow of $2510 \text{ m}^3 \text{ s}^{-1}$, which is around three times higher than flood threshold
439 ($Q = 845 \text{ m}^3 \text{ s}^{-1}$).

440 The generalized floods of 2001–2002 at the Andancette station (water flow of $4780 \text{ m}^3 \text{ s}^{-1}$) and the
441 Isère ($928 \text{ m}^3 \text{ s}^{-1}$) and Gardon ($6700 \text{ m}^3 \text{ s}^{-1}$) rivers was identified at 102 cm depth in the sediment core.
442 The geochemical modeling results based on the total and non-reactive fractions were similar for the
443 Ardèche (7% and 8%, respectively), Durance (11% and 8%) and Gardon (37% and 43%) rivers. Based
444 on the occurrence of a generalized flood at Andancette station, the contribution obtained with the non-
445 reactive concentrations (19%) was more relevant than the contribution estimated using the total
446 fraction (5%). The SPM contribution from the Isère River was estimated at 23% based on the non-
447 reactive fraction. Contributions modeled for the Gardon River could only be validated based on past
448 flooding events because of the absence of hydro-sedimentary data for this period. The SPM
449 contributions of the Gardon River for the total and non-reactive fractions (37% and 43%, respectively)
450 are consistent with the reported water flow of $6700 \text{ m}^3 \text{ s}^{-1}$, which is around six times higher than the
451 flood threshold ($Q = 402 \text{ m}^3 \text{ s}^{-1}$). Consequently, based on the SPM source contributions modeled here
452 for the Middle Rhône and Isère rivers, the non-reactive fraction appears to be more relevant than the
453 total fraction for tracing the SPM contributions of this major event.

454 The sediments deposited in 1996 (131 cm depth) reflect the SPM inputs during a Cévenol flood.
455 According to the 10-yr flood of the Ardèche River, which reached a maximum water flow of 1780 m^3
456 s^{-1} , the estimated SPM contribution for this tributary was very small (0.5%). Results obtained for the

457 sediment core showed that, based on the total fraction, the Isère and Gardon rivers were the main SPM
458 contributors at 36% and 39%, respectively, while SPM inputs from the Durance, Ardèche and Middle
459 Rhône rivers were much lower (19%, 0.5% and 6%, respectively). In contrast, the modeling performed
460 with the non-reactive concentrations resulted in more relevant estimates than using the total
461 concentrations, with contributions of 9% from the Ardèche River and 33% from the Gardon River.
462 However, it is possible that the geochemical signatures (based on the tracers selected) of the Gardon
463 and Ardèche rivers were not clearly distinct, which would suggest that part of the SPM inputs from the
464 Ardèche River would be assimilated as inputs from the Gardon River. For this type of hydrological
465 event, Zebracki et al. (2015) estimated that the contributions were similar between the upstream
466 tributaries (31%; Andancette station, Isère), the pre-alpine tributaries (30%; Durance), and the
467 Cévenol tributaries (39%; Ardèche, Gardon). According to these results, the estimated SPM
468 contributions of the Durance River in the 1996 layer are more similar using the non-reactive fraction
469 (23%) than the total fraction (19%). Moreover, by combining the estimated contributions for
470 Andancette station and Isère River, the contribution for the non-reactive fraction (35%) was similar to
471 the value estimated by Zebracki et al. (2015) (31%), in contrast to our geochemical modeling with the
472 total concentrations (42%).

473 In 1993 and 1994 (i.e., at 142–151 cm depth), there were three extensive Mediterranean floods that led
474 to moderate floods of the Isère River and the Middle Rhône at Andancette and high water flows for the
475 southern tributaries (peaks of $2350 \text{ m}^3 \text{ s}^{-1}$ and $4340 \text{ m}^3 \text{ s}^{-1}$ for the Durance and Ardèche rivers,
476 respectively). Therefore, the main expected SPM contributions are probably those of the Ardèche and
477 the Durance rivers. As the only hydrological data available for the Gardon River was the occurrence of
478 a 10-yr flood in 1993 (DREAL, 2011), it was not possible to validate the SPM contribution of this
479 tributary. Geochemical modeling with the total fraction resulted in a major contribution from the
480 Durance River (45%). In contrast to expected results, the Isère River had a larger relative SPM
481 contribution (29%) than the Ardèche River (15%). Geochemical modeling with the non-reactive
482 fraction confirmed the Durance River as the main source of SPM (75%), followed by the Ardèche
483 River (13%). Moreover, SPM inputs from the Isère River were lower using the non-reactive fraction

484 (7%) than for the total fraction (29%), which once again suggests that the results obtained with the
485 non-reactive fraction are more reliable than results obtained with the total fraction.

486 Finally, in 1990 (184 cm depth), the Rhône was subjected to a very intense oceanic flood that
487 particularly affected the tributaries located upstream of the city of Lyon (Upper Rhône River) with
488 peak water flows of $4310 \text{ m}^3 \text{ s}^{-1}$ and $1040 \text{ m}^3 \text{ s}^{-1}$ for the Middle Rhône and Isère River, respectively.
489 Our estimates modeled using the total fraction showed that the Isère and Gardon rivers were the main
490 contributors to SPM inputs at the outlet of the Rhône River basin and that the other three tributaries
491 supplied less than 4% sediment each. In contrast, contribution estimates modeled using the non-
492 reactive fraction were equivalent between the Isère River (37%) and the Middle Rhône (37%), which
493 better reflects the SPM inputs of the major event studied. For this flooding event, the results modeled
494 from the non-reactive fraction are therefore more reliable than the results obtained with the total
495 fraction.

496

497 **4. Conclusion**

498 To overcome the non-conservative behavior of metals, we used the metal concentrations in the non-
499 reactive fraction of SPM/sediments on a sediment core collected at the outlet of the Rhône basin, a site
500 for which no information on the historical SPM contributions was available. This study focused on the
501 estimation of tributary contributions over the last 40 yr using a geochemical modeling approach. We
502 demonstrated that estimations of SPM contributions were significantly influenced by past
503 anthropogenic inputs responsible for an increase in total Zn concentrations in the deepest layers of the
504 sediment core. In fact, the range test selected Zn as a conservative tracer even though it is highly
505 reactive in the deepest layers of the sediment core, which may bias the results of contribution
506 modeling based on the total fraction. Based on a comparison with the results of Zebracki et al. (2015),
507 who used radionuclide data on SPM, it is clear that the results obtained with the non-reactive fraction
508 are closer to those obtained by Zebracki et al. (2015) compared to contributions estimated using the
509 total fraction. Indeed, using the non-reactive fraction, we showed that the main SPM contributor over

510 the 1981–2013 period was the Durance River. Moreover, the detailed study of major past flooding
511 events showed that our estimates of tributary SPM contributions were more reliable and consistent
512 when the non-reactive metal concentrations were used, especially to trace SPM sources in the deepest
513 layers of the sediment core. Therefore, when concentrations of a geochemical element are influenced
514 by anthropogenic inputs, as for investigations relative to historical SPM inputs, it is more relevant to
515 use the non-reactive fraction rather than the total fraction. This study demonstrated that our original
516 fingerprinting method based on the non-reactive fraction of metals in SPM/sediment is a robust tool
517 for estimating source contributions in a sediment core, as it removed the influence of past
518 anthropogenic inputs on tracer concentrations. Furthermore, this fingerprinting approach made it
519 possible, for the first time in the Rhône River basin, to reconstruct the historical contributions of the
520 main tributaries during major flooding events. It would now be instructive to apply this method to
521 SPM/sediments in coastal environments or those affected by significant past anthropogenic inputs
522 (e.g., rivers influenced by mining activities).

523 Thus, this fingerprinting method using the residual fraction at the Rhône River basin scale allows to:

- 524 - Increase the number of available tracers after the range test of SPM sources, as demonstrated by
525 Begorre et al. (2021),
- 526 - Remove the influence of past anthropogenic inputs of metals such as Zn,
- 527 - Provide results that are more relevant when comparing with available hydrological and
528 sedimentary data,
- 529 - Provide information on the major sources of sediments that are exported into the Mediterranean
530 Sea that could impact its ecosystems.

531 In terms of recommendations for future studies, as presented by Begorre et al. (2021), the use of total
532 metal concentrations, especially when they are highly reactive, is problematic. Indeed, source
533 fingerprinting using total concentrations of metals must be applied only for metals with low reactivity
534 to improve estimation of SPM source contributions. Therefore, before applying source fingerprinting in
535 a river basin, it is necessary to investigate metal reactivity to avoid the use of high-reactive metals.

536 Finally, we highly recommend using tracers in the non-reactive fraction when sources and target samples
537 were not sampled at the same period (e.g., with a difference of more than 5 or 10 yr).

538

539 **Acknowledgements**

540 This study was supported by the Rhône Sediment Observatory (OSR), a multi-partner research
541 program partly funded by the 'Plan Rhône' and by the European Regional Development Fund
542 (ERDF). We thank the partner organizations that provided data to the OSR database especially for this
543 study: CNR (Compagnie Nationale du Rhône), FOEN (Federal Office of the Environment,
544 Switzerland), Grand Lyon city council, Veolia, DREAL (the French hydrological agency), and EDF
545 (Electricité de France). This study is also part of the ArcheoRhône project, which was funded by the
546 Agence de l'Eau Rhône Méditerranée Corse. We thank our INRAE colleagues Lysiane Dherret,
547 Ghislaine Grisot, Alexandra Gruat, Loïc Richard, Mickaël Lagouy and Fabien Thollet, and our IRSN
548 colleagues Franck Giner and David Mourier for their invaluable assistance with core sampling, SPM
549 sampling, field campaigns, sample treatment and analyses, and Yoann Copard (Université de Rouen)
550 for his help with COP analysis on the sediment core.

551

552 **References**

- 553 Appleby, P.G., 1998. Dating recent sediments by ^{210}Pb : problems and solutions. *Stuk A-145*, 7–24
- 554 Audry, S., Schäfer, J., Blanc, G., Jouanneau, J.M., 2004. Fifty-year sedimentary record of heavy metal
555 pollution (Cd, Zn, Cu, Pb) in the Lot River reservoirs (France). *Environmental Pollution* 132, 413–
556 426. DOI: 10.1016/j.envpol.2004.05.025
- 557 Bégorre, C., Dabrin, A., Morereau, A., Lepage, H., Mourier, B., Masson, M., Eyrolle, F., Coquery,
558 M., 2021. Relevance of using the non-reactive geochemical signature in sediment core to estimate
559 historical tributary contributions. *J Environ Management* 292, 112775.
560 DOI: 10.1016/j.jenvman.2021.112775

561 Chen, F. X., Fang, N. F., Wang, Y. X., Tong, L. S., Shi, Z. H., 2017. Biomarkers in sedimentary
562 sequences: Indicators to track sediment sources over decadal timescales. *Geomorphology* 278, 1-11.
563 DOI: 10.1016/j.geomorph.2016.10.027

564 Collins, A.L., Walling, D.E., Leeks, G.J.L., 1997. Use of the geochemical record preserved in
565 floodplain deposits to reconstruct recent changes in river basin sediment sources. *Geomorphology* 19,
566 151–167. DOI: 10.1016/S0169-555X(96)00044-X

567 Collins, A.L., Pulley, S., Foster, I.D.L., Gellis, A., Porto, P., Horowitz, A.J., 2017. Sediment source
568 fingerprinting as an aid to catchment management: A review of the current state of knowledge and a
569 methodological decision-tree for end-users. *Journal of Environmental Management* 194, 86–108.
570 DOI: 10.1016/j.jenvman.2016.09.075

571 Dabrin, A., Schäfer, J., Bertrand, O., Masson, M., Blanc, G., 2014. Origin of suspended matter and
572 sediment inferred from the residual metal fraction: Application to the Marennes Oleron Bay, France.
573 *Continental Shelf Research* 72, 119–130. DOI: 10.1016/j.csr.2013.07.008

574 Dabrin, A., Bégorre, C., Bretier, M., Dugué, V., Masson, M., Le Bescond, C., Le Coz, J., Coquery, M.,
575 2021. Reactivity of particulate element concentrations: apportionment assessment of suspended
576 particulate matter sources in the Upper Rhône River, France. *J Soils Sediments* 21, 1256–1274. DOI:
577 10.1007/s11368-020-02856-0

578 Delile, H., Masson, M., Miège, C., Le Coz, J., Poulier, G., Le Bescond, C., Radakovitch, O., Coquery,
579 M., 2020. Hydro-climatic drivers of land-based organic and inorganic micropollutant fluxes: the
580 regime of the largest river water inflow of the Mediterranean Sea. *Water Research* 185, 116067. DOI:
581 10.1016/j.watres.2020.116067

582 Dendeviel, A.M., Mourier, B., Dabrin, A., Delile, H., Coynel, A., Gosset, A., Liber, Y., Berger, J.F.,
583 Bedell, J.P., 2020. Metal pollution trajectories and mixture risk assessment along a major European
584 river since the 1960s (Rhône River, France). *Environment International* 144, 106032. DOI:
585 10.1016/j.envint.2020.106032

586 Dhivert, E., Grosbois, C., Courtin-Nomade, A., Bourrain, X., Desmet, M., 2016. Dynamics of metallic
587 contaminants at a basin scale — Spatial and temporal reconstruction from four sediment cores (Loire
588 fluvial system, France). *Science of the Total Environment* 541, 1504–1515.
589 DOI: 10.1016/j.scitotenv.2015.09.146

590 DREAL, 2011. Evaluation préliminaire des risques d’inondation sur le bassin Rhône-Méditerranée-
591 Partie IV: Unité de présentation “Haut-Rhône”. 42 p. (In French).

592 Ferrand, E., Eyrolle, F., Radakovitch, O., Provansal, M., Dufour, S., Vella, C., Raccasi, G., Gurriaran,
593 R., 2012. Historical levels of heavy metals and artificial radionuclides reconstructed from overbank
594 sediment records in lower Rhône River (South-East France). *Geochimica et Cosmochimica Acta* 82,
595 163-182. DOI: 10.1016/j.gca.2011.11.023

596 Foucher, A., Chaboche, P.A., Sabatier, P., Evrard, O., 2021. A worldwide meta-analysis (1977–2020)
597 of sediment core dating using fallout radionuclides including ^{137}Cs and $^{210}\text{Pb}_{\text{xs}}$. *Earth Syst.Sci. Data* 13,
598 4951–4966. DOI: 10.5194/essd-13-4951-2021

599 Gateuille, D., Owens, P., Petticrew, E., Booth, B., French, T., Déry, S., 2019. Determining
600 contemporary and historical sediment sources in a large drainage basin impacted by cumulative
601 effects: the regulated Nechako River, British Columbia, Canada. *Journal of Soils and Sediments* 19.
602 DOI: 10.1007/s11368-019-02299-2

603 Gellis, A.C., Noe, G.B., 2013. Sediment source analysis in the Linganore Creek watershed, Maryland,
604 USA, using the sediment fingerprinting approach: 2008 to 2010. *Journal of Soils and Sediments* 13,
605 1735–1753. DOI: 10.1007/s11368-013-0771-6

606 Haddadchi, A., Ryder, D.S., Evrard, O., Olley, J., 2013. Sediment fingerprinting in fluvial systems:
607 review of tracers, sediment sources and mixing models. *International Journal of Sediment Research*
608 28, 560–578. DOI: 10.1016/S1001-6279(14)60013-5

609 Henkel, S., Mogollón, J.M., Nöthen, K., Franke, C., Bogus, K., Robin, E., Bahr, A., Blumenberg, M.,
610 Pape, T., Seifert, R., März, C., de Lange, G.J., Kasten, S., 2012. Diagenetic barium cycling in Black

611 Sea sediments – A case study for anoxic marine environments. *Geochimica et Cosmochimica Acta* 88,
612 88–105. DOI: 10.1016/j.gca.2012.04.021

613 Huang, D., Du, P., Walling, D.E., Ning, D., Wei, X., Liu, B., Wang, J., 2019. Using reservoir deposits
614 to reconstruct the impact of recent changes in land management on sediment yield and sediment
615 sources for a small catchment in the Black Soil region of Northeast China. *Geoderma* 343, 139–154.
616 DOI: 10.1016/j.geoderma.2019.02.014

617 Hughes, A.O., Olley, J.M., Croke, J.C., McKergow, L.A., 2009. Sediment source changes over the last
618 250 years in a dry-tropical catchment, central Queensland, Australia. *Geomorphology* 104, 262–275.
619 DOI: 10.1016/j.geomorph.2008.09.003

620 ISO, 1995. ISO 10694, Soil quality – Determination of organic and total carbon after dry combustion
621 (elementary analysis).

622 ISO, 2009. ISO 13320, Particle size analysis – Laser diffraction methods.

623 Liu, H.C., You, C.F., Huang, B.J., Huh, C.A., 2013. Distribution and accumulation of heavy metals in
624 carbonate and reducible fractions of marine sediment from offshore mid-western Taiwan. *Marine
625 Pollution Bulletin* 73, 37-46. DOI: 10.1016/j.marpolbul.2013.06.007

626 Manjoro, M., Rowntree, K., Kakembo, V., Foster, I., Collins, A.L., 2017. Use of sediment source
627 fingerprinting to assess the role of subsurface erosion in the supply of fine sediment in a degraded
628 catchment in the Eastern Cape, South Africa. *Journal of Environmental Management* 194, 27–41.
629 DOI: 10.1016/j.jenvman.2016.07.019

630 Masson, M., Angot, H., Le Bescond, C., Launay, M., Dabrin, A., Miège, C., Le Coz, J., Coquery, M.,
631 2018. Sampling of suspended particulate matter using particle traps in the Rhône River: Relevance and
632 representativeness for the monitoring of contaminants. *Science of the Total Environment* 637–638,
633 538–549. DOI: 10.1016/j.scitotenv.2018.04.343

634 Morereau, A., Lepage, H., Claval, D., Cossonnet, C., Ambrosi, J.P., Mourier, B., Winiarski, T.,
635 Copard, Y., Eyrolle, F., 2020. Trajectories of technogenic tritium in the Rhône River (France). *Journal*
636 *of Environmental Radioactivity* 223–224, 106370. DOI: 10.1016/j.jenvrad.2020.106370

637 Mourier, B., Desmet, M., Van Metre, P., Mahler, B., Perrodin, Y., Roux, G., Bedell, J.P., Lefèvre, I.,
638 Babut, M., 2014. Historical records, sources, and spatial trends of PCBs along the Rhône River
639 (France). *The Science of the total environment* 476-477C, 568-576.
640 DOI: 10.1016/j.scitotenv.2014.01.026

641 Navratil, O., Evrard, O., Esteves, M., Ayrault, S., Lefèvre, I., Legout, C., Reyss, J.L., Gratiot, N.,
642 Nemery, J., Mathys, N., Poirel, A., Bonté, P., 2012. Core-derived historical records of suspended
643 sediment origin in a mesoscale mountainous catchment: the River Bléone, French Alps. *Journal of*
644 *Soils and Sediments* 12, 1463–1478. DOI: 10.1007/s11368-012-0565-2

645 Ollivier, P., Radakovitch, O., Hamelin, B., 2011. Major and trace element partition and fluxes in the
646 Rhône River. *Chemical Geology* 285, 15–31. DOI: 10.1016/j.chemgeo.2011.02.011

647 Owens, P.N., Walling, D.E., Leeks, G.J.L., 1999. Use of floodplain sediment cores to investigate
648 recent historical changes in overbank sedimentation rates and sediment sources in the catchment of the
649 River Ouse, Yorkshire, UK. *CATENA* 36, 21–47. DOI: 10.1016/S0341-8162(99)00010-7

650 Owens, P.N., Blake, W.H., Gaspar, L., Gateuille, D., Koiter, A.J., Lobb, D.A., Petticrew, E.L.,
651 Reiffarth, D.G., Smith, H.G., Woodward, J.C., 2016. Fingerprinting and tracing the sources of soils
652 and sediments: Earth and ocean science, geoarchaeological, forensic, and human health applications.
653 *Earth-Science Reviews* 162, 1–23. DOI: 10.1016/j.earscirev.2016.08.012

654 Poulhier, G., Launay, M., Le Bescond, C., Thollet, F., Coquery, M., Le Coz, J., 2019. Combining flux
655 monitoring and data reconstruction to establish annual budgets of suspended particulate matter,
656 mercury and PCB in the Rhône River from Lake Geneva to the Mediterranean Sea. *Science of The*
657 *Total Environment* 658, 457-473. DOI: 10.1016/j.scitotenv.2018.12.075

658 Pulley, S., Foster, I., Antunes, P., 2015. The application of sediment fingerprinting to floodplain and
659 lake sediment cores: assumptions and uncertainties evaluated through case studies in the Nene Basin,
660 UK. *Journal of Soils and Sediments* 15, 2132–2154. DOI: 10.1007/s11368-015-1136-0

661 Pulley, S., Van der Waal, B., Rowntree, K., Collins, A.L. 2018. Colour as reliable tracer to identify the
662 sources of historically deposited flood bench sediment in the Transkei, South Africa: A comparison
663 with mineral magnetic tracers before and after hydrogen peroxide pre-treatment. *CATENA* 160, 242–
664 251. DOI: 10.1016/j.catena.2017.09.018

665 Thollet, F.; Le Bescond, C.; Lagouy, M.; Gruat A.; Grisot, G.; Le Coz, J.; Coquery, M.; Lepage, H.;
666 Gairoard, S.; Gattacceca, J.C.; Ambrosi, J.-P.; Radakovitch, O., Dur, G., Richard, L., Giner, F.,
667 Eyrolle, F., Angot, H., Mourier, D., Bonnefoy, A., Dugué, V., Launay, M., Troudet, L., Labille, J.,
668 Kieffer, L. (2021): Rhône Sediment Observatory (OSR); INRAE.
669 <https://dx.doi.org/10.17180/OBS.OSR>Torres Astorga, R., de los Santos Villalobos, S., Velasco, H.,
670 Domínguez-Quintero, O., Pereira Cardoso, R., Meigikos dos Anjos, R., Diawara, Y., Dercon, G.,
671 Mabit, L., 2018. Exploring innovative techniques for identifying geochemical elements as fingerprints
672 of sediment sources in an agricultural catchment of Argentina affected by soil erosion. *Environmental*
673 *Science and Pollution Research* 25, 20868–20879. DOI: 10.1007/s11356-018-2154-4

674 Van der Waal, B., Rowntree, K., Pulley, S., 2015. Flood bench chronology and sediment source
675 tracing in the upper Thina catchment, South Africa: the role of transformed landscape connectivity.
676 *Journal of Soils and Sediments* 15, 2398-2411. DOI: 10.1007/s11368-015-1185-4

677 Vauclin, S., Mourier, B., Dendievel, A.M., Marchand, P., Vénisseau, A., Morereau, A., Lepage, H.,
678 Eyrolle, F., Winiarski, T., 2021. Temporal trends of legacy and novel brominated flame retardants in
679 sediments along the Rhône River corridor in France. *Chemosphere* 271, 129889. DOI:
680 10.1016/j.chemosphere.2021.129889

681 Walling, D.E., 2005. Tracing suspended sediment sources in catchments and river systems. *Science of*
682 *the Total Environment* 344, 159–184. DOI: 10.1016/j.scitotenv.2005.02.011

683 Wang, W., Fang, N., Shi, Z., Lu, X., 2018. Prevalent sediment source shift after revegetation in the
684 Loess Plateau of China: Implications from sediment fingerprinting in a small catchment. *Land*
685 *Degradation & Development* 29, 3963-3973. DOI: 10.1002/ldr.3144

686 Wynants, M., Millward, G., Patrick, A., Taylor, A., Munishi, L., Mtei, K., Brendonck, L., Gilvear, D.,
687 Boeckx, P., Ndakidemi, P., Blake, W. H., 2020. Determining tributary sources of increased
688 sedimentation in East-African Rift Lakes. *Science of The Total Environment* 717, 137266. DOI:
689 10.1016/j.scitotenv.2020.137266

690 Zebracki, M., Eyrolle-Boyer, F., Evrard, O., Claval, D., Mourier, B., Gairoard, S., Cagnat, X.,
691 Antonelli, C., 2015. Tracing the origin of suspended sediment in a large Mediterranean river by
692 combining continuous river monitoring and measurement of artificial and natural radionuclides.
693 *Science of the Total Environment* 502, 122–132. DOI: 10.1016/j.scitotenv.2014.08.082

Fig. 1: Location of sampling sites for SPM sources (Middle Rhône River at Andancette station, Isère, Ardèche, Gardon, Durance river stations of the Rhône Sediment Observatory - OSR network) and sediment core (Mas des Tours at the outlet of the Rhône River).

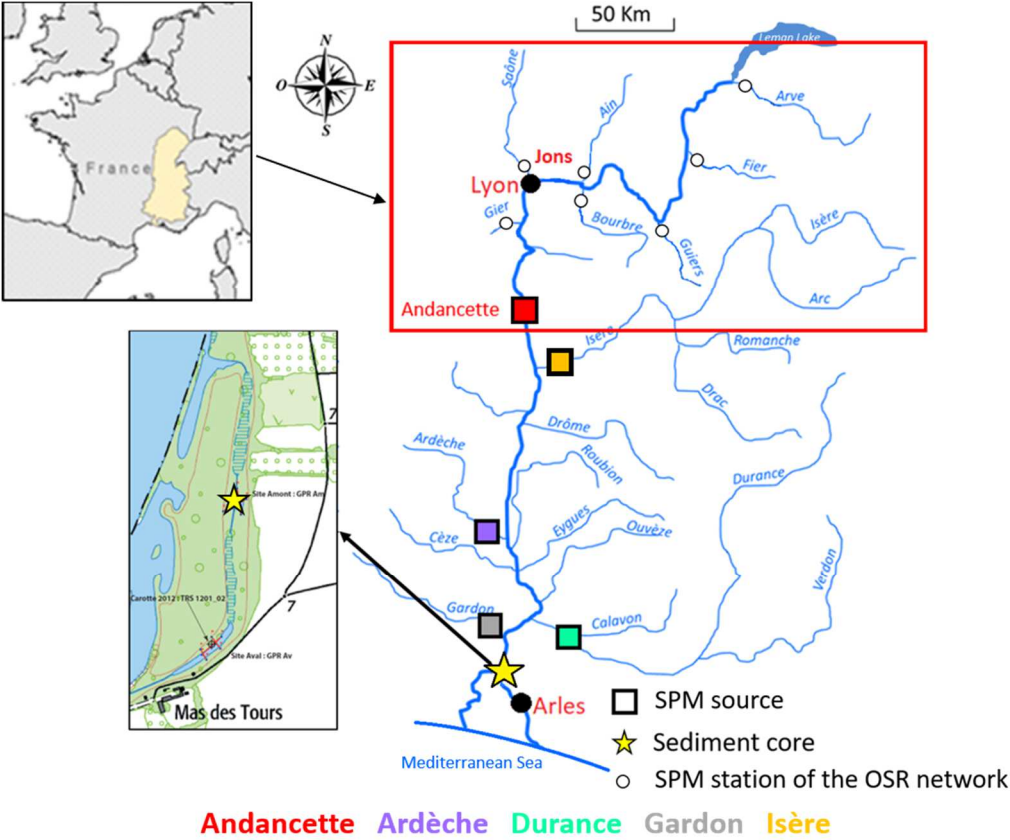
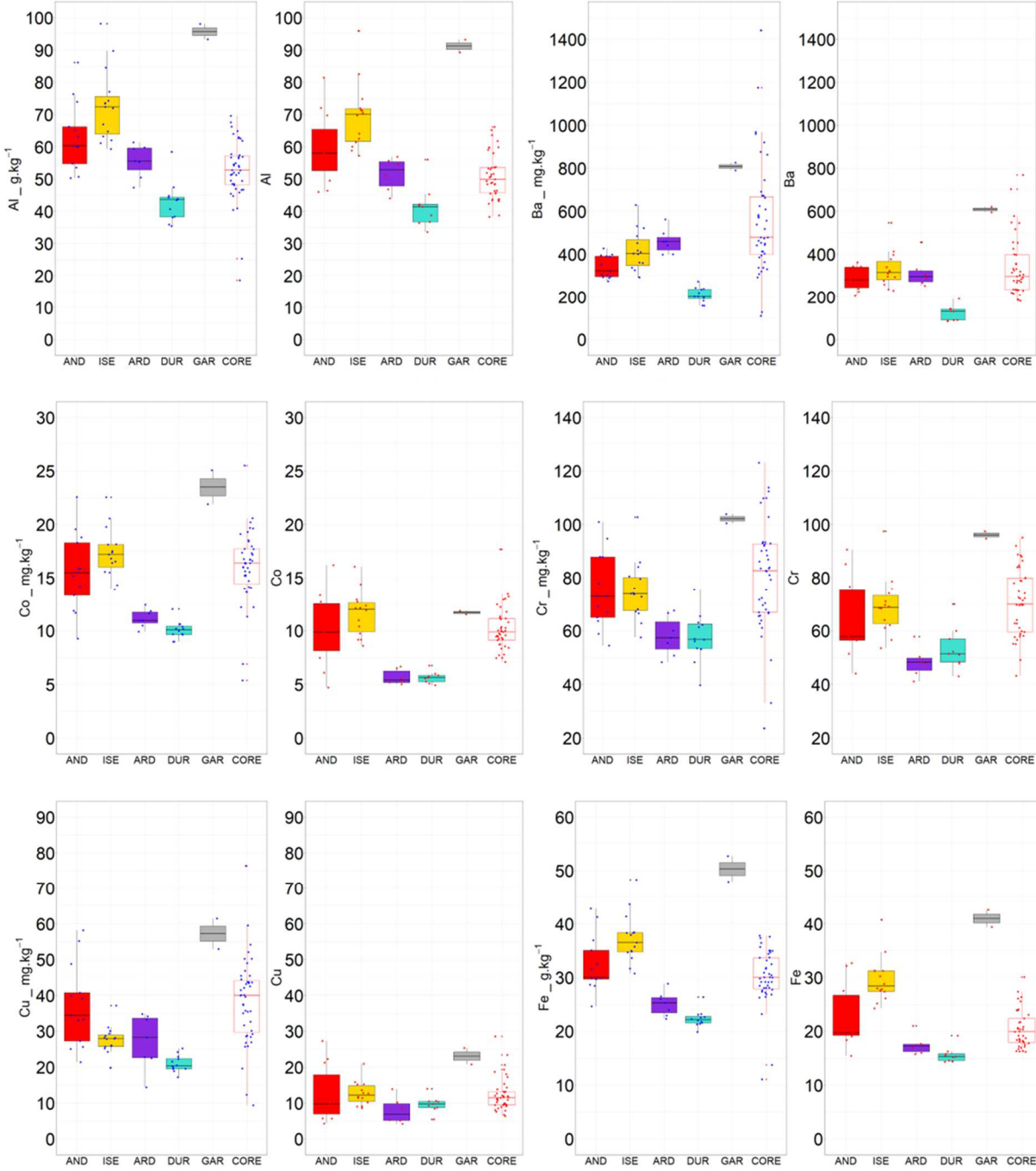


Fig. 2: Metal concentrations (non-corrected data by particle size) measured in the total (blue on the left) and non-reactive (red on the right) fractions of SPM in the Rhône River (Middle Rhône River station at Andancette - AND) and four tributaries (Isère –ISE, Ardèche – ARD, Durance- DUR, Gardon- GAR) and in the sediment core sampled in the Rhône at Mas des Tours site.



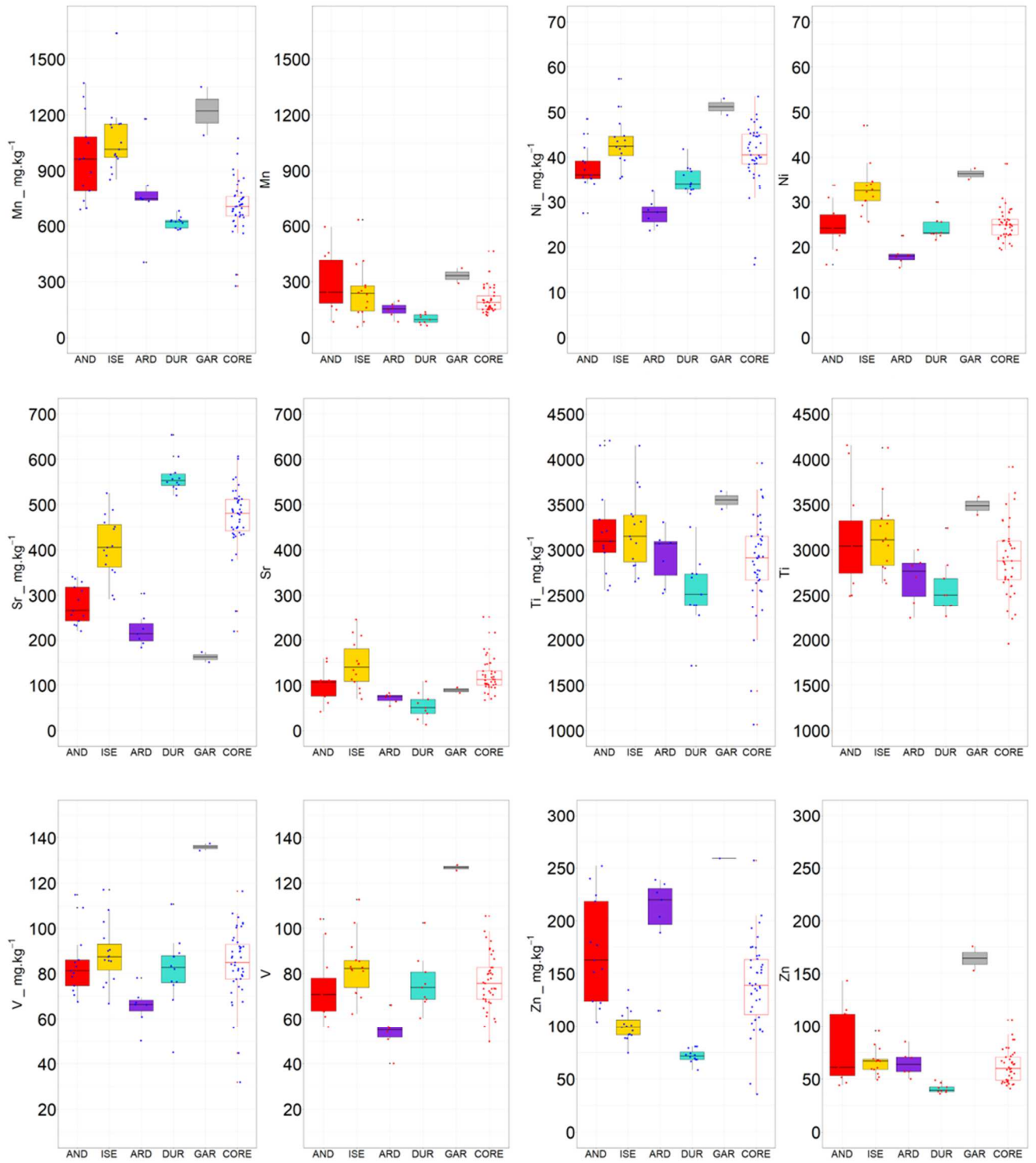
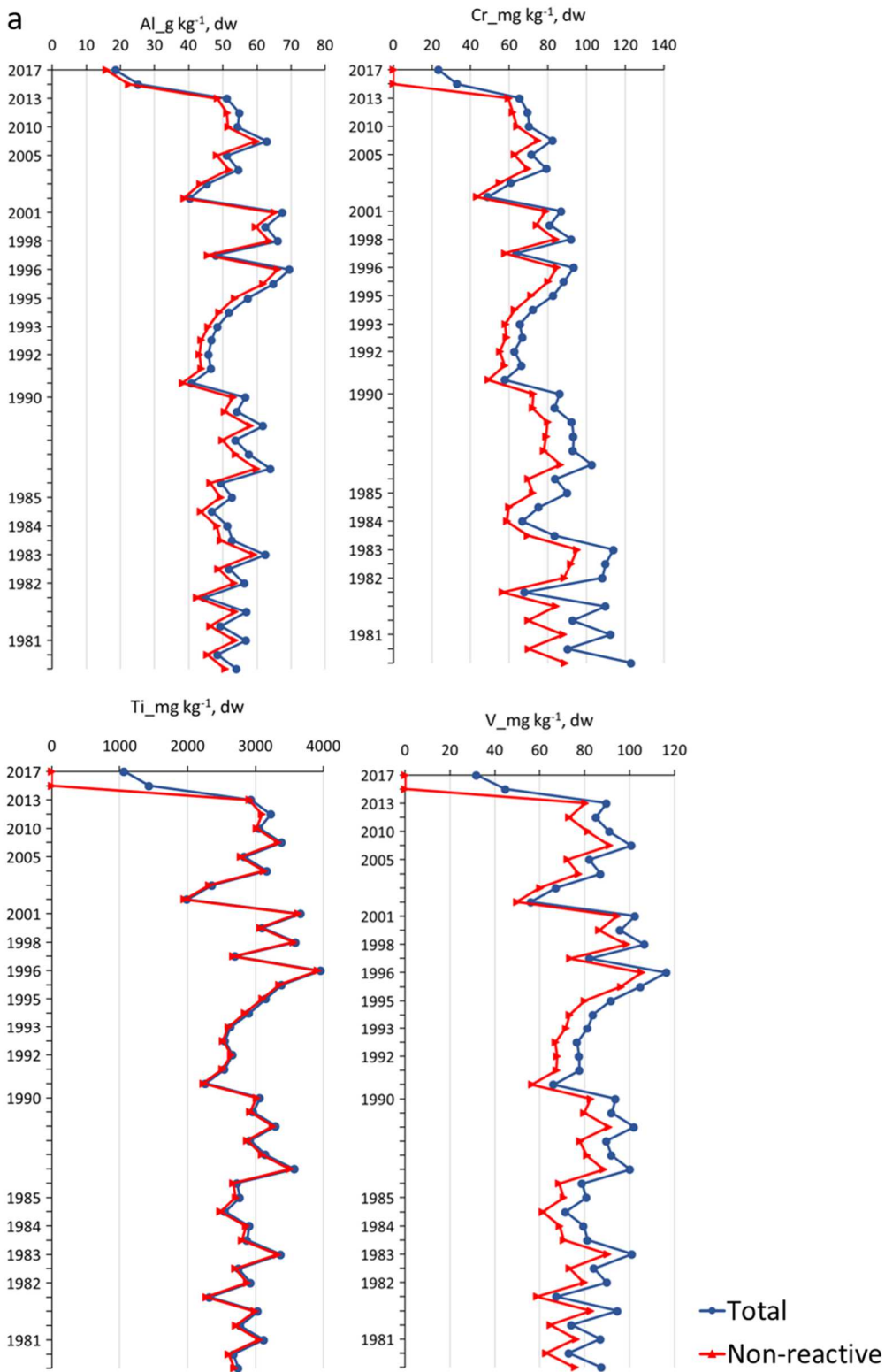
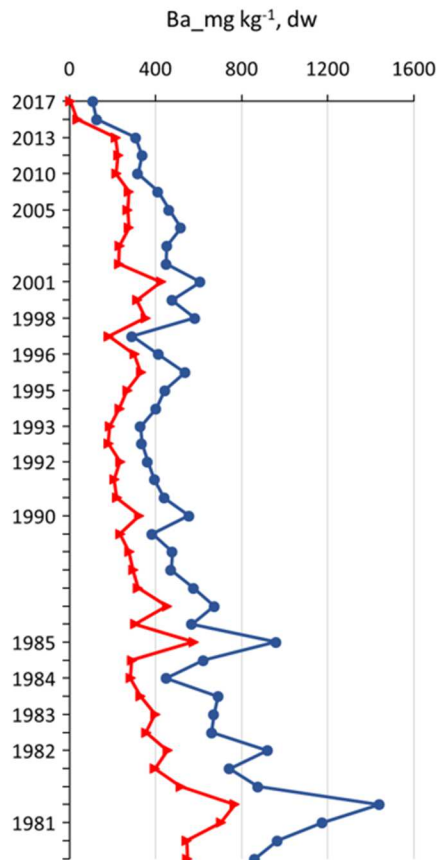
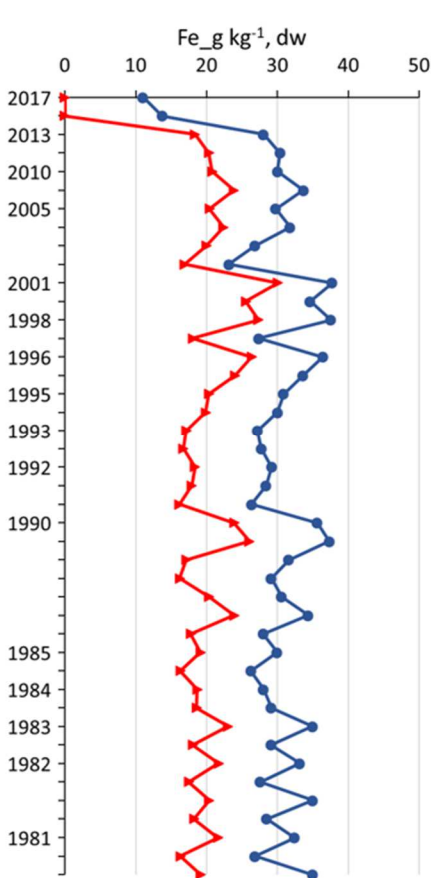
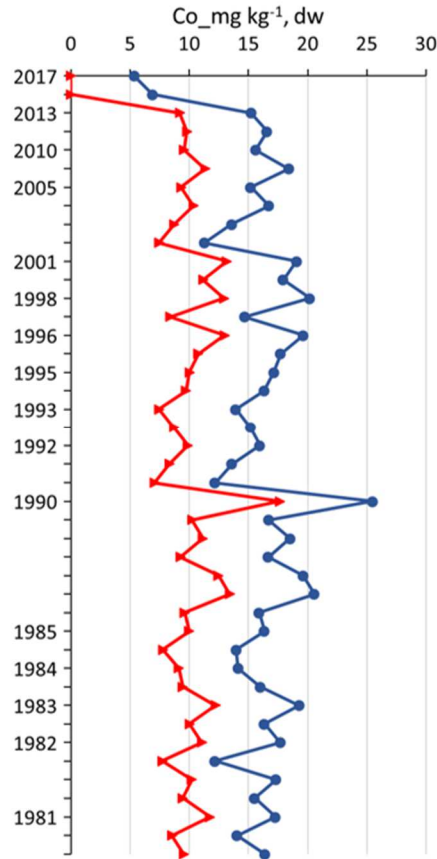
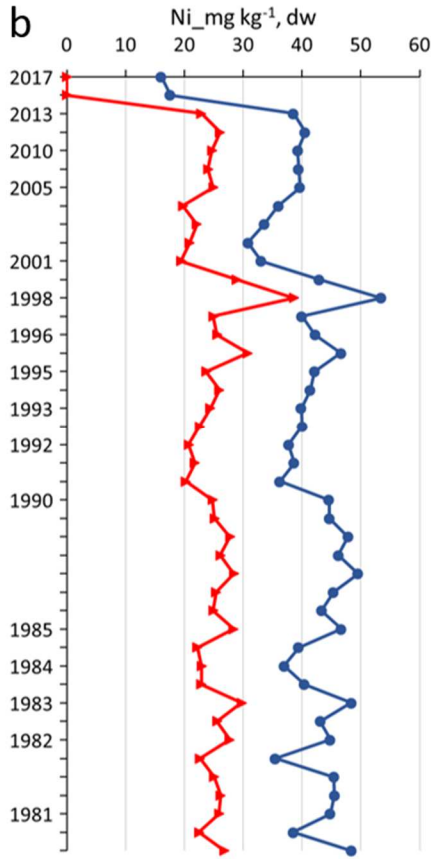


Fig. 3: Metal concentrations in the sediment core sampled in the Rhône at Mas des Tours site. The three identified groups represent metals that are not reactive (a), moderately reactive (b) and highly reactive (c). Example of three behaviours of metals along the sediment core by comparing concentrations in the total (blue line) and non-reactive (red line) fractions.



b



C

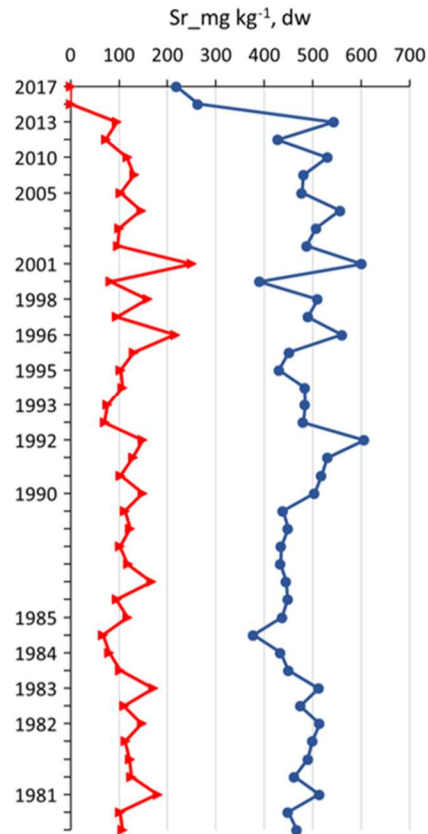
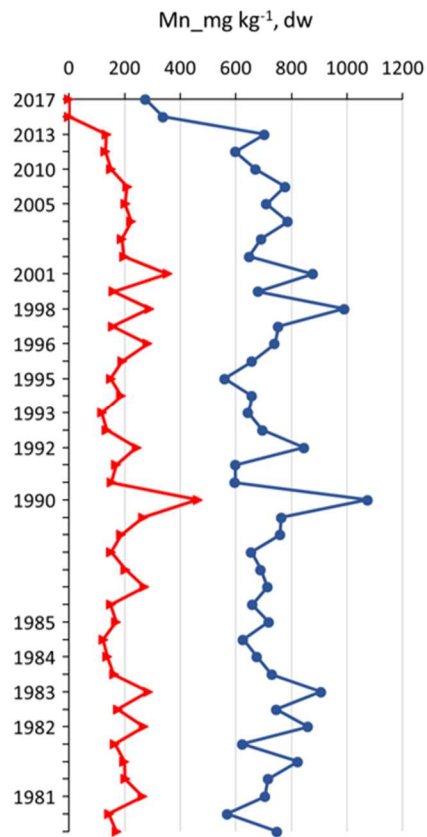
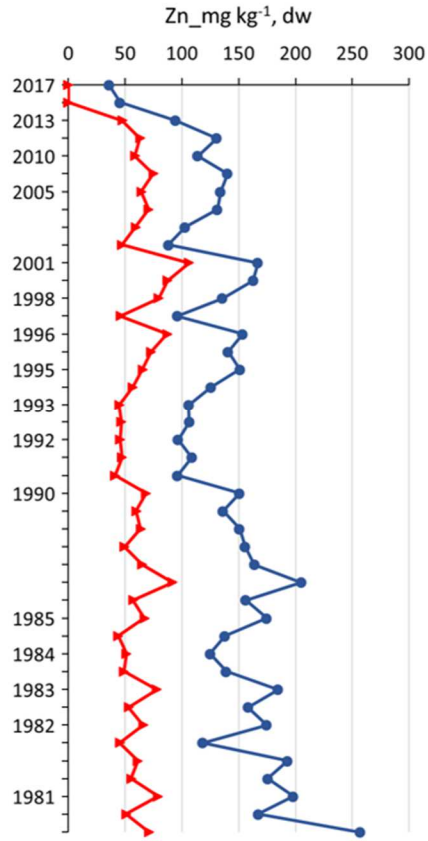
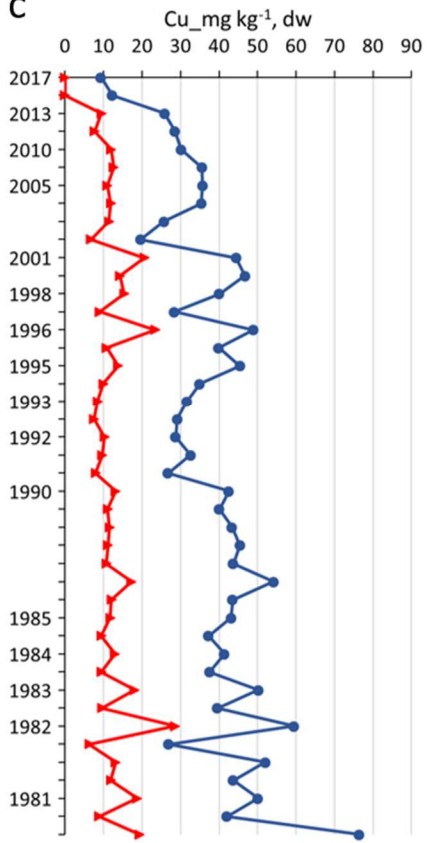


Fig. 4: Profile of source apportionment modelling by using tracers in the total (a) and non-reactive (b) fractions, in sediment core at Mas des Tours site, from 1981 to 2013. The black line represents the 1990 layer. Main historical flooding events ($\text{m}^3 \text{s}^{-1}$) are reported for the Upper Rhône River and each tributary over the 30-yr period (c)

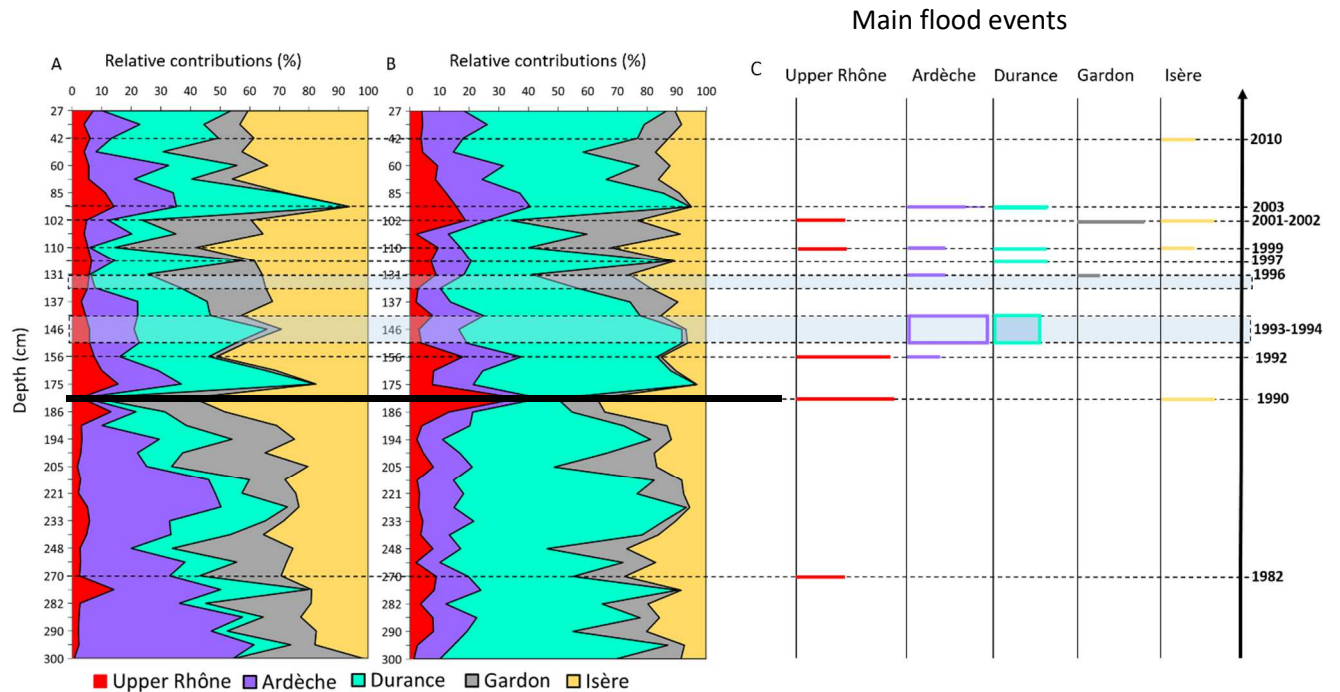


Fig. 5: Principal component analysis (PCA) performed using selected tracer concentrations in the total (a) and non-reactive (b) fractions of SPM at the Rhône River Middle station (Andancette) and tributaries. The concentrations of the tracers used are corrected for particle size. PCA shows correlations (or no correlation) between total (a) or non-reactive (b) concentrations and source contributions.

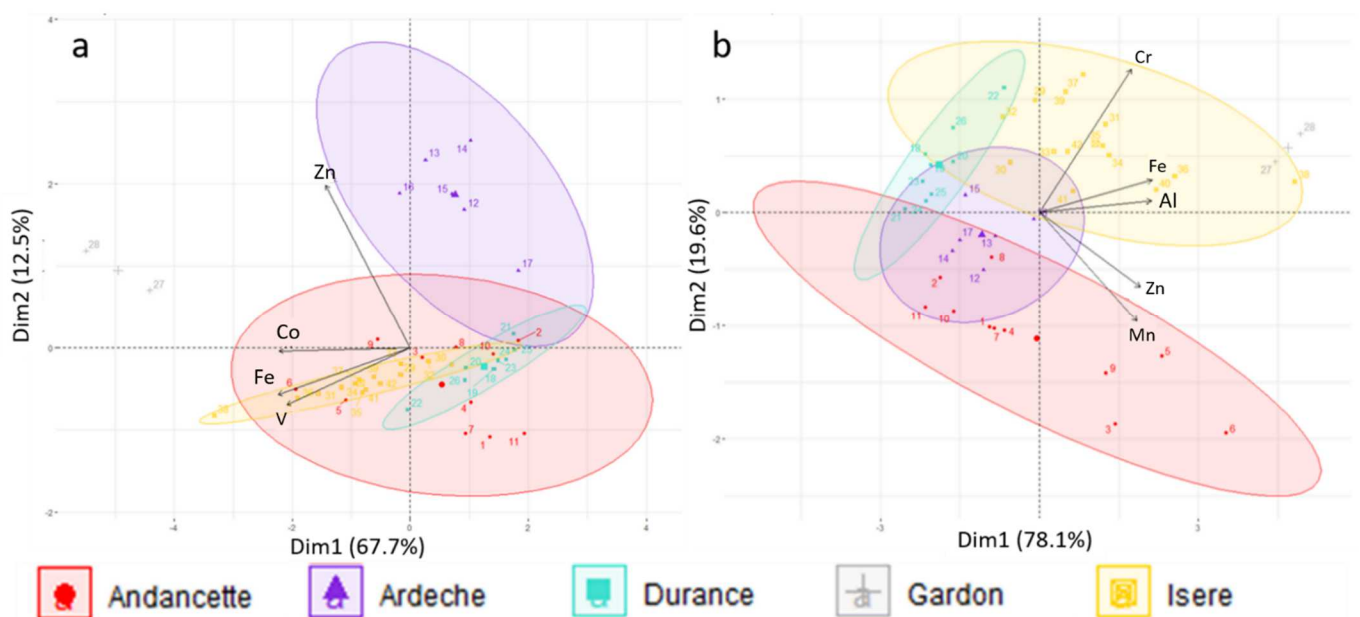


Table 1: Summary of sampling periods for each tributary and associated hydro-sedimentary conditions.

Tributary	N =42 samples	Water flow (m³ s⁻¹)	SPM concentration (mg L⁻¹)
Middle Rhône River (Andancette station)	11 (flood: 3, base flow: 8)	263 - 1040 (2018-2019 period)	3.5 - 18.8 (2019)
Isère	14 (flood: 3, base flow: 11)	175 – 671 (2014-2018)	6.75 – 1488 (2014-2018)
Ardèche	6 (flood: 1, base flow: 5)	9 - 459 (2016)	1.7 - 13.8 (2016)
Gardon	2 (flood: 1, base flow: 1)	- (2017)	- (2017)
Durance	9 (flood: 2, base flow: 7)	38 – 1613 (2011-2016)	6.2 - 545 (2014-2016)

Table 2: Proportions (in %) of the reactive fraction compared to the total fraction for each trace and major elements. The results are presented for the SPM tributaries and for the sediment core samples divided in two main periods (1991-2013 and 1981-1990).

Elements	Proportions of the reactive fraction (%)						
	Middle Rhône	Isère	Ardèche	Durance	Gardon	Sediment core (1991-2013)	Sediment core (1981-1990)
Al	7±1	3.0±0.5	7.2±0.5	4.5±0.5	4.7±0.5	5.3±0.9	6.3±0.5
Ba	18±4	19±3	32±6	40±8	25±4	39±7	43±6
Co	38±7	32±5	48±6	43±5	50±6	39±4	38±4
Cr	14±3	7±1	16±4	9±1	5.9±0.3	11±2	18±4
Cu	68±9	54±7	68±10	55±8	60±1	66±7	72±6
Fe	31±6	19±2	30±2	30±3	19±1	32±5	37±5
Mn	72±10	76±11	78±7	82±7	72±9	73±6	72±7
Ni	35±5	23±3	33±3	31±2	29.0±0.2	39±5	42±3
Sr	66±9	64±9	66±7	89±7	45.2±0.1	76±7	74±5
Ti	3±1	0.7±0.1	8±2	0.4±0.1	1.8±0.2	1.5±0.7	2.0±0.4
V	13±2	5±1	17±2	10±1	6.7±0.2	11±2	13±1
Zn	56±7	33±6	65±7	43±5	42±1	50±6	63±5

Table 3: Statistical results for tracer selection procedure, which combines the range test, the Kruskal-Wallis test (KW, $p < 0.05$) and the discriminant factor analysis (DFA), for total and non-reactive fractions of SPM sources. The “V” shows the geochemical tracers that are retained at each step and “X” shows those that fail. For the range test, the number of layers, for which metals failed the range test, are indicated in parenthesis. For DFA, the “X” shows the metals removed from the procedure while the metals retained are characterised by a value representing the discriminatory power of the selected tracers.

Elements	Total fraction			Non-reactive fraction		
	Range test	KW test	DFA	Range test	KW test	DFA
Al	V	V	X	V	V	1.00
Ba	X (5 layers)	X	X	X (2 layers)	X	X
Co	V	V	0.55	V	V	X
Cr	X (1 layer)	X	X	V	V	0.95
Cu	X (1layer)	X	X	V	V	X
Fe	V	V	0.95	V	V	0.62
Mn	V	V	X	V	V	0.98
Ni	V	V	X	V	V	X
Sr	V	V	X	V	V	X
Ti	X (1 layer)	X	X	X (1 layer)	X	X
V	V	V	1.00	V	V	X
Zn	V	V	0.88	V	V	0.81

Supplementary material

Fig. SI.1: Box-and-whisker plot of median grain size (D50, values in μm) in SPM tributaries (Upper Rhône River station at Andancette – AND, Isère –ISE, Ardèche – ARD, Durance- DUR, Gardon- GAR) and in the sediment core sampled in the Rhône at Mas des Tours site.

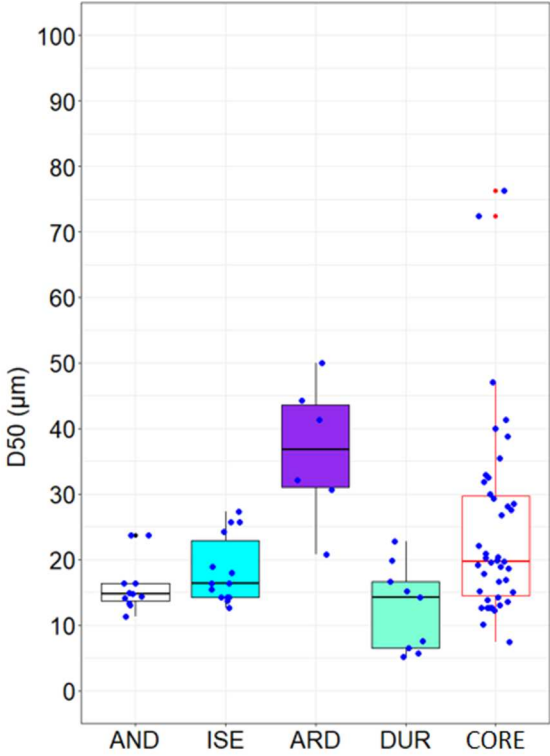


Fig. S1.2: Profile of median particle size (D50; μm) in the sediment core.

